

Exploring the Accuracy Limits of Local Pair Natural Orbital Coupled-Cluster Theory

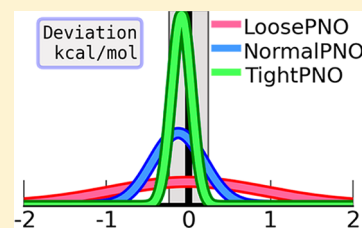
Dimitrios G. Liakos,[†] Manuel Sparta,[†] Manoj K. Kesharwani,[‡] Jan M. L. Martin,[‡] and Frank Neese^{*,†}

[†]Max Planck Institute for Chemical Energy Conversion, Stiftstrasse 32-34, 45470 Mülheim an der Ruhr, Germany

[‡]Department of Organic Chemistry, Weizmann Institute of Science, 76100 Rehovot, Israel

S Supporting Information

ABSTRACT: The domain based local pair natural orbital coupled cluster method with single-, double-, and perturbative triple excitations (DLPNO-CCSD(T)) is an efficient quantum chemical method that allows for coupled cluster calculations on molecules with hundreds of atoms. Because coupled-cluster theory is the method of choice if high-accuracy is needed, DLPNO-CCSD(T) is very promising for large-scale chemical application. However, the various approximations that have to be introduced in order to reach near linear scaling also introduce limited deviations from the canonical results. In the present work, we investigate how far the accuracy of the DLPNO-CCSD(T) method can be pushed for chemical applications. We also address the question at which additional computational cost improvements, relative to the previously established default scheme, come. To answer these questions, a series of benchmark sets covering a broad range of quantum chemical applications including reaction energies, hydrogen bonds, and other noncovalent interactions, conformer energies, and a prototype organometallic problem were selected. An accuracy of 1 kcal/mol or better can readily be obtained for all data sets using the default truncation scheme, which corresponds to the stated goal of the original implementation. Tightening of the three thresholds that control DLPNO leads to mean absolute errors and standard deviations from the canonical results of less than 0.25 kcal/mol (<1 kJ/mol). The price one has then to pay is an increased computational time by a factor close to 3. The applicability of the method is shown to be independent of the nature of the reaction. On the basis of the careful analysis of the results, three different sets of truncation thresholds (termed “LoosePNO”, “NormalPNO”, and “TightPNO”) have been chosen for “black box” use of DLPNO-CCSD(T). This will allow users of the method to optimally balance performance and accuracy.



1. INTRODUCTION

Among the available ab initio quantum mechanical methods, the hierarchy of coupled-cluster (CC) approaches stands out as being particularly accurate and robust.¹ The coupled-cluster model with single and double substitutions (CCSD) corrected by perturbative triples (CCSD(T)) has, in fact, become the “gold standard” of computational chemistry.^{2–4} However, the tremendous computational expenses associated with the solution of the canonical procedure make it impossible to adopt CCSD(T) for routine applications.

To overcome this limitation, several groups have developed approximations that reduce the computational cost of the method while preserving its accuracy. The most successful strategies are rooted in the locality of the electron correlation and, although each implementation is unique, the attempts can be divided loosely into two complementary classes. In the first class, the system of interest is partitioned into fragments and the total correlation is approximated by the sum of each fragment contribution. Early applications of this strategy are due to Förner and co-workers^{5,6} and Stoll and co-workers.^{7,8} Subsequently, this approach has been adopted by Fedorov and Kitaura (fragment molecular-orbital CC),⁹ Li and Li (divide-and-conquer),¹⁰ Jørgensen and co-workers (divide-expand-consolidate),^{11,12} Piecuch and co-workers and Kallay and co-workers (cluster-in-molecule),^{13–15} as well as by Friedrich and

co-workers (incremental CC).^{16–18} Within the second class, the entire system is treated at once. The first attempts to exploit the locality of electron correlation in this manner are due to Pulay and Saebø, who introduced the concepts of local correlation domains and projected atomic orbitals (PAO).^{19–23} Elaborating on these concepts, a variety of correlation methods have been developed and implemented by Werner and Schütz,^{24–30} Ayala and Scuseria,³¹ and Head-Gordon and co-workers.^{32–34} Finally, methods that implement orbital specific virtual orbitals (OSVs) should be mentioned.^{24,29,35–38}

In recent years, our group has been active in the development of correlation methods using the concept of the local pair natural orbital (LPNO).^{39–41} The PNO approach is firmly rooted in the pioneering work of Meyer, Kutzelnigg, Ahlrichs, Staemmler, and co-workers^{42–54} and has recently regained popularity after it became apparent that it is the preferred basis for local correlation calculations.^{35,37,55} The LPNO family of methods has been successfully used to investigate the mechanism of prochiral enamide hydrogenation,⁵⁶ the equilibrium between the peroxo and bis-(μ -oxo) isomers of $[\text{Cu}_2(\text{en})_2(\text{O})_2]^{2+}$,⁵⁷ weakly bound molecular

Received: December 15, 2014

systems,⁵⁸ and it is found to be a reliable source of data for basis set extrapolation schemes.⁵⁹ However, the inherent fifth-order scaling (for LPNO–CCSD) made the method expensive for molecules with more than ~100 atoms. Hence, the LPNO–CCSD method was completely redesigned by combining the concept of PNOs and PAOs. The resulting domain-based local pair natural orbital CCSD (DLPNO–CCSD) was reported to be near linear scaling.⁶⁰ Further extension of the method by adding quasiperturbative treatment of the triple excitations yielded to the DLPNO–CCSD(T) model.⁶¹ The largest coupled cluster calculations reported to date involving more than 600 atoms, and almost 9000 basis functions have been achieved on the basis of the DLPNO–CCSD and DLPNO–CCSD(T) schemes.⁶¹ Recently, DLPNO–CCSD(T) has been employed in the study of the catalytic cycle of the asymmetric hydrogenation of olefins promoted by phosphino-oxazoline iridium complexes, thus demonstrating the potential of the methods for routine application to chemical phenomena.⁶² The LPNO and DLPNO methods^{39–41,60,61} were designed to provide results that are within about 1 kcal/mol of the canonical results (for a recent review we refer to ref 63). While an accuracy of this kind is certainly good enough for a large variety of chemical applications, it is interesting to investigate the question how far the accuracy of the local correlation treatment can be realistically pushed while still realizing significant to spectacular savings relative to canonical correlation calculations. This question is best addressed by systematic benchmark calculations on large data sets of reference reaction and interaction energies. In recent years, many of such benchmark sets have been established. For example, Pople and co-workers,^{64,65} Truhlar and co-workers,^{66–72} and Grimme and co-workers^{73–79} have developed databases covering a broad spectrum of physical and chemical properties to assess and validate electronic structure methods.

In this article, we explore the accuracy limits of the DLPNO–CCSD(T) method, by applying it to four benchmark sets. The first benchmark set consists of 51 reaction energies for which accurate results have been published recently by Friedrich and Hänchen.⁸⁰ The second benchmark set (S66) focuses on noncovalent intermolecular interactions.^{81,82} The last two benchmark sets consist of the conformers of melatonin^{83–86} and butane-1,4-diol.

2. THEORETICAL BACKGROUND

The theory of the DLPNO–CCSD(T) method has been described in detail in recent publications,^{60,61} here we only mention the most important features in order to document the truncation parameters and other aspects that would be investigated in this work. In an effort to explore the accuracy limits of DLPNO–CCSD(T), we investigated the effect of the truncation parameters; how the use of the semicanonical local MP2 impacts the pair selection, an alternative scheme for the truncation of the PNO space based on energy rather than occupation numbers, the inclusion of triple excitations involving two weak pairs, and the use of spin-component scaled MP2 (SCS-MP2)⁸⁷ to partition the pairs into strongly and weakly interacting and to devise corrections for the truncations.

2.1. The DLPNO–CCSD(T) Method. Like essentially all other local correlation methods, the DLPNO–CCSD(T) treatment starts with a single determinant reference wave function, often the Hartree–Fock determinant. In the initial step, we localize the occupied orbitals of the reference

determinant, by default using the Foster–Boys scheme.⁸⁸ We then obtain the correlation energy as a sum over electron pair correlation energies ϵ_{ij} , where labels i and j refer to localized occupied orbitals. The pair correlations are inherently of local nature and fall off very quickly with the distance between the orbital centers of orbitals i and j . Hence, electron pairs with expected negligible contributions (weak pairs) can be excluded from the treatment, thus leaving a linear scaling number of electron pairs (strong pairs) to be treated in the local correlation treatment. In DLPNO–CCSD(T), the selection of strong and weak pairs is achieved in two steps. First a prescreening based on a multipole estimate (computationally highly efficient) of the pair correlation energy is conducted. For the surviving pairs, the semicanonical local MP2 (SC-LMP2) pair correlation energy is computed and, if this energy is above the threshold T_{CutPairs} (default value = 10^{-4} Eh), the pair is included in the subsequent coupled-cluster treatment. The criterion for computing the SC-LMP2 energy is that the multipole estimate should be larger than 0.01 times T_{CutPairs} . PNOs are constructed from the SC-LMP2 pair densities and expanded in terms of the PAOs of a large domain that is used in SC-LMP2 calculation. PNOs with occupation numbers larger than T_{CutPNO} (default value = 3.33×10^{-7}) are kept. This construction leads to a tremendous compaction of the wave function at the expense of introducing a separate set of correlating orbitals for each electron pair. The SC-LMP2 pair correlation energies are also used to estimate the error due to the local pair and PNO approximations and the correction is added to the coupled-cluster correlation energy to obtain the final estimate. The final truncation parameter T_{CutMKN} (default value = 10^{-3}) determines the size of the initial domain in which the PNOs are expanded. Atoms that have Mulliken population larger than T_{CutMKN} for a given localized MO i are included in the primary domain of orbital i . Pair domains are constructed by unification of the domains of the individual orbitals. For the many additional technical details involved in the realization of the LPNO and DLPNO methods, we refer to the original literature.^{39–41,60,61}

2.2. Semicanonical Local MP2 vs Full Local MP2. As part of their local correlation scheme, Werner, Schütz, and co-workers commonly employ a full local MP2 (LMP2) scheme²⁸ rather than a semicanonical one (SC-LMP2). In the present work, we have investigated whether such LMP2 scheme (which is fully invariant with respect to the choice of internal orbitals) can improve the accuracy of the DLPNO–CCSD(T) scheme. Briefly, SC-LMP2 approximates the MP2 energy by ignoring the off-diagonal terms of the Fock matrix (arising from the localization of the internal orbitals). Conversely, LMP2 recovers, by means of an iterative procedure, the canonical MP2 energy for a set of localized orbitals. According to variational Hylleraas method, the MP2 energy can be obtained by minimization of the appropriate Hylleraas functional:⁸⁹

$$E_{\text{MP2}} = \min_t \{ 2 \langle \Psi_1 | \hat{H} | \Psi_0 \rangle + \langle \Psi_0 | \hat{H}_0 - E_0 | \Psi_1 \rangle \}$$

where \hat{H}_0 is the zeroth-order Hamiltonian, $|\Psi_0\rangle$ is the reference determinant, $|\Psi_1\rangle$ is the first-order wave function, and E_0 the reference energy. The quantity t collectively denotes the MP2 amplitudes. Rewriting the MP2 energy as an explicit functional of the MP2 amplitudes leads to the equation:

$$E_{\text{MP2}}[t] = \left\{ \frac{1}{2} \sum_{ijab} \langle ij||ab \rangle t_{ab}^{ij} - \frac{1}{2} \sum_{ijkab} F_{kj} t_{ab}^{ij} t_{ab}^{ik} + \frac{1}{2} \sum_{ijabc} F_{cb} t_{ab}^{ij} t_{ac}^{ij} \right\}$$

where the indices ij,k and a,b,c denote occupied and virtual orbitals, respectively, and F denotes the Fock matrix. Differentiation of the MP2 Hylleraas energy functional with respect to the MP2 amplitudes gives

$$\frac{\partial E_{\text{MP2}}}{\partial t_{ab}^{ij}} = 2R_{ab}^{ij}$$

where R_{ab}^{ij} is the MP2 residual

$$R_{ab}^{ij} = \langle ij||ab \rangle - \sum_k (t_{ab}^{kj} F_{ki} + t_{ab}^{ik} F_{kj}) + \sum_c (t_{ac}^{ij} F_{bc} + t_{cb}^{ij} F_{ac})$$

Thus, vanishing of the MP2 residual determines the MP2 amplitudes that fulfill the Hylleraas variation criteria. Our implementation largely follows the original description of the method by Pulay and Saebø^{23,90} as efficiently implemented and improved by Werner, Schütz, and co-workers.²⁸ We mention in passing that the LMP2 algorithm needs to be carefully designed in order to not become the dominant part of the entire DLPNO-CCSD(T) scheme. The high cost arises from the large domains that are included in the DLPNO-CCSD(T) scheme and the correspondingly large PAO spaces that need to be treated in the LMP2 (528 PAOs for the most expensive part for the benzene dimer with cc-pVTZ). Specific details of our implementation will be published elsewhere.

2.3. Energy-Based Selection of the PNOs. There are potentially many ways in which PNOs can be constructed and selected. Construction schemes according to Meyer⁵⁰ as well as from semicanonical MP2 amplitudes have been explored in the original work and both lead to very similar results.⁴⁰ We have also tested PNOs defined as eigenfunctions of the symmetrized exchange operators $1/2(\mathbf{K}^{ij} + \mathbf{K}^{ji})$. However, these PNOs perform significantly worse than the default choice. Finally, we also investigated the possibility to select the PNOs (calculated in the standard way from semicanonical MP2 pair densities) by their estimated energy contribution. In a nutshell, for a given pair (ij) and PNO \tilde{a}_{ij} , this increment is given by $1/(1 + \delta_{ij}) T_{\tilde{a}_{ij}\tilde{a}_{ij}}^{ij} K_{\tilde{a}_{ij}\tilde{a}_{ij}}^{ij}$. There is clearly a strong connection between the energy selection defined in this way and the occupation number selection because the pair density is essentially $\mathbf{D}^{ij} = \mathbf{T}^{ij}\mathbf{T}^{ij+} + \mathbf{T}^{ij+}\mathbf{T}^{ij}$, and the amplitudes are related to the exchange operators through $T_{\tilde{a}_{ij}\tilde{b}_{ij}}^{ij} = K_{\tilde{a}_{ij}\tilde{b}_{ij}}^{ij}/(\varepsilon_{\tilde{a}_{ij}} + \varepsilon_{\tilde{b}_{ij}} - F_{ii} - F_{jj})$.

3. COMPUTATIONAL DETAILS

The ORCA⁹¹ suite of programs was used for all calculations referenced in this article. The basis sets used were the ones from the cc-pVnZ^{92,93} family of basis sets with n ranging from 2 to 3, depending on the data set. For the S66 interaction energies, all calculations were counterpoise corrected.⁹⁴ The correlation fitting basis sets (cc-pVnZ/C in ORCA nomenclature) that were developed by Hättig and co-workers⁹⁵ have been used for DLPNO-CCSD calculations. In the investigation of the complete basis set (CBS) limit by means of extrapolation techniques, the two-point scheme (EP-1)^{96–98} was adopted.

All computations were performed on a cluster of 18 nodes. Each node is equipped with 4 Intel Xeon E7-8837 2.67 GHz eight-core CPU, 256 GB RAM, and a single hard disk of 5 TB. For each of the cc-pVDZ and cc-pVTZ calculations, two and four cores were allocated, respectively.

While the CCSD energy is invariant to unitary transformation of the occupied and virtual orbitals respectively, the triples correction is usually based on a canonical representation. To avoid iterative processes, the DLPNO-CCSD(T) triples correction is designed to reproduce a semicanonical treatment of the triples in which the occupied orbitals are localized and the virtual orbitals are canonical. In this approximation, diagonal Fock matrix elements F_{ii} replace the orbital energies ε_i of the localized orbitals. This treatment is usually referred to as “ T_0 ” by Schütz, Werner, and co-workers.^{24,26} As documented in the Supporting Information (Figure S1–2), differences between canonical CCSD(T) and CCSD(T_0) reaction energies are typically small (on average <0.2 kcal/mol), but they can reach up to 1 kcal/mol in some cases. There is, however, no evidence that CCSD(T_0) is in worse agreement with experiment than CCSD(T) once pushed to the basis set limit.⁹⁹ Because DLPNO-CCSD(T) models the T_0 treatment, our reference values all refer to canonical CCSD(T_0) using the same localized internal orbitals as in the DLPNO calculations but avoiding any truncations.

3.1. The Benchmark Sets. The first benchmark set consists of 51 reaction energies for which accurate results have been recently published by Friedrich and Hänchen,⁸⁰ hereafter the FH data set. The database covers a large set of chemically interesting processes such as isomerizations (3-methylpentane \rightarrow dimethylbutane), hydrogenations (1-hexene + $\text{H}_2 \rightarrow n$ -hexane), allylic shifts (1-pentene \rightarrow *trans*-2-pentene), and oxidations ($\text{C}_4\text{H}_9\text{CHO} + \text{H}_2\text{O}_2 \rightarrow \text{C}_4\text{H}_9\text{CO}_2\text{H} + \text{H}_2\text{O}$). The 51 reaction energies that constitute the FH data set require the calculation of 81 molecules. At least one of the moieties involved in each reaction is a medium size molecule (the limiting factor for the canonical CC reference calculations), for example, $\text{CO}(\text{NHC}_3\text{H}_7)_2$ has 26 atoms for a total of 524 basis functions at cc-pVTZ. The reference reaction energy was used to sort the data set, for example, reaction1 ($\text{C}_6\text{H}_{12}\text{O} + 2\text{H}_2\text{O}_2 \rightarrow \text{ethyl-}\gamma\text{-butyrolactone} + 3\text{H}_2\text{O}$) and reaction 51 ($\text{C}_3\text{H}_7\text{CO}_2\text{H} + \text{NH}_3 \rightarrow \text{C}_3\text{H}_7\text{CONH}_2 + \text{H}_2\text{O}$) have a reference value of -153.2 and -0.2 kcal/mol, respectively.

The S66 database, developed by P. Hobza and co-workers, comprises of 66 molecular complexes (e.g., Figure 1), where

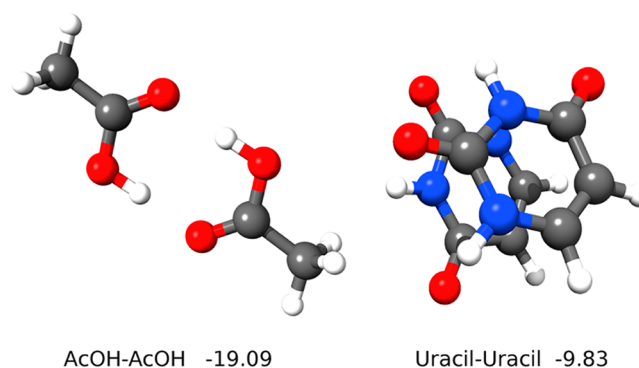


Figure 1. Acetic acid and uracil dimers: examples of the molecular complexes in the S66 database. Interaction energies are given in kcal/mol (ref 81).

hydrogen bonds, dispersion interactions, aliphatic–aliphatic, and π –aliphatic interactions play a crucial role.^{81,82} These interactions are commonly found in biomolecular structures, therefore S66 is suited for testing the accuracy of methods when applied to biochemical systems.⁸¹ Within the S66 set of molecules, three broad subgroups of interaction energies are recognized by design. The first subgroup contains mainly electrostatic-rich interactions. On the basis of the reference values of the original publication, the largest absolute interaction energy is reaction 22. Here, acetamide (CH_3CONH_2) interacts with uracil ($\text{C}_4\text{H}_4\text{N}_2\text{O}_2$) through hydrogen bonds. For the calculation of the adduct using the modest cc-pVTZ basis set, one needs 472 basis functions, this already is an expensive calculation for any normal computer if canonical CCSD(T) is employed. The complexes in the second subgroup are dominated by dispersion interactions: π – π stacking, aliphatic–aliphatic, and π –aliphatic. In this subgroup, reaction 44 (ethene–pentane) is the one with the largest interaction energy (4.46 kcal/mol). For the product one would need, again using the cc-pVTZ basis set, 434 basis functions. Finally, in the remaining complexes, denoted in the original publication as “mixed”, both types of interaction coexist.

The last two data sets deal with the conformational energies of butane-1,4-diol and melatonin. Butane-1,4-diol is a versatile chemical intermediate in the production of polymers and tetrahydrofuran,¹⁰⁰ and it can be biotechnologically produced by microbial conversion of renewable feedstock.¹⁰¹ For this molecule, 65 gas phase conformers were identified at MP2 level of theory¹⁰² (see Figure 2). For the conformers of butane-1,4-

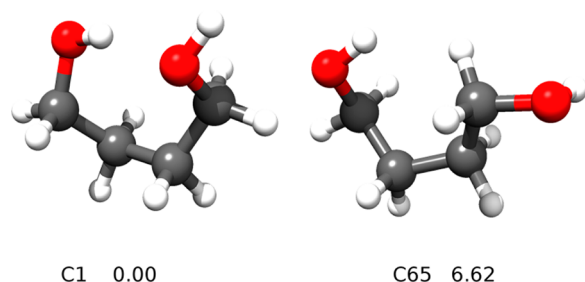


Figure 2. Most and least stable of the butane-1,4-diol conformers (relative energy in kcal/mol, ref 102).

diol, we used the cc-pVDZ and cc-pVTZ basis sets for consistency (134 and 320 basis functions, respectively). Thus, this molecule is certainly manageable from the computational effort point of view and given the fact that it presents different forms of intramolecular hydrogen bonds it constitutes an ideal candidate for a benchmark study of hydrogen bonds and isomerization barriers in organic molecules. The conformational energies range from 0 to almost 7 kcal/mol.

Melatonin (*N*-acetyl-5-methoxytryptamine) is a human endocrine hormone that regulates the circadian day–night rhythm and seasonal biorhythm by the classical chronobiology¹⁰³ and it is involved in a variety of biological functions.¹⁰⁴ The flexibility of the molecule gives rise to a rich conformational space (four conformers are shown in Figure 3), where the relative energies of the conformers are due to intramolecular weak hydrogen bonds and quadrupole–dipole aromatic–amide interactions.⁸³ The first database of melatonin conformers was published by Tasi and co-workers,⁸⁴ who investigated the conformational space with the Hartree–Fock (HF) method using a double- ζ basis set. Subsequently, the data

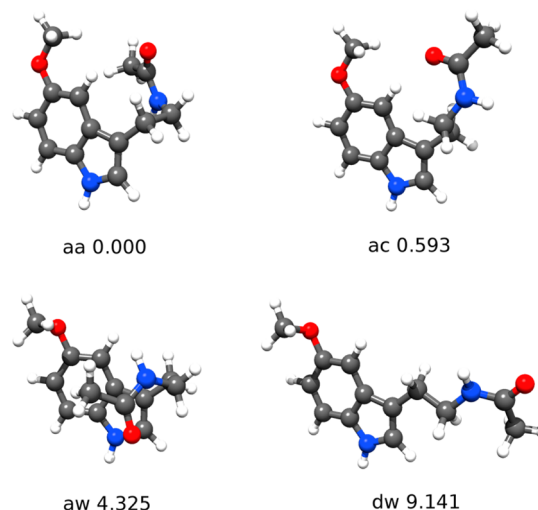


Figure 3. Four representative conformers of melatonin and their relative energies in kcal/mol computed by Martin and co-workers (ref 86).

set was revised and the effect of electron correlation was accounted for with second-order perturbation theory (MP2).⁸⁵ Finally, Martin and co-workers obtained high quality energies for the 52 conformers of melatonin by means of explicitly correlated ab initio methods.⁸⁶

In melatonin, all of the effects observed on the S66 set and the butane-1,4-diol coexist. In fact, melatonin presents intramolecular weak hydrogen bonds (in the same fashion as butane-1,4-diol) in addition to quadrupole–dipole aromatic–amide interactions (showing similarities with the “mixed” interactions of the S66 set). Each molecule consists of 33 atoms, and their descriptions require a total of 318 and 734 basis functions when cc-pVDZ and cc-pVTZ are employed, respectively. Although this does not pose issues for DLPNO–CCSD(T), the canonical CCSD(T)/cc-pVTZ counterparts are computationally demanding calculations. Considering that the conformational energies converge slowly with respect to basis set extension,⁸⁶ this is a good example of why accurate and efficient ab initio correlated methods like DLPNO–CCSD(T) are needed.

4. RESULTS AND DISCUSSION

To assess the accuracy of the DLPNO–CCSD(T) method, we first study the convergence of the DLPNO–CCSD(T) results with respect to the three main thresholds and investigate the use of SC-LMP2 and LMP2. Subsequently, three default sets of thresholds based on the balance of accuracy and efficiency will be presented and evaluated using the previously defined benchmark data sets. Finally, we comment on the use of spin-component scaled MP2 (SCS-MP2) and on the number of weak pairs included in the triple excitations.

4.1. Convergence with Respect to Truncation Thresholds. The convergence of the DLPNO–CCSD(T) reaction energies of the FH data set with respect to the three parameters is shown in Figure 4, using the cc-pVDZ basis set. Similar results were obtained using aug-cc-pVDZ basis set (Supporting Information, Figure S36). The statistical analysis was conducted with respect to reference values obtained with CCSD(T_0). We note that extremely tight DLPNO calculations ($T_{\text{CutPairs}} = 0$, $T_{\text{CutPNO}} = 10^{-10}$, and $T_{\text{CutMKN}} = 0$) converge to the reference values as shown by the average error and standard deviation of

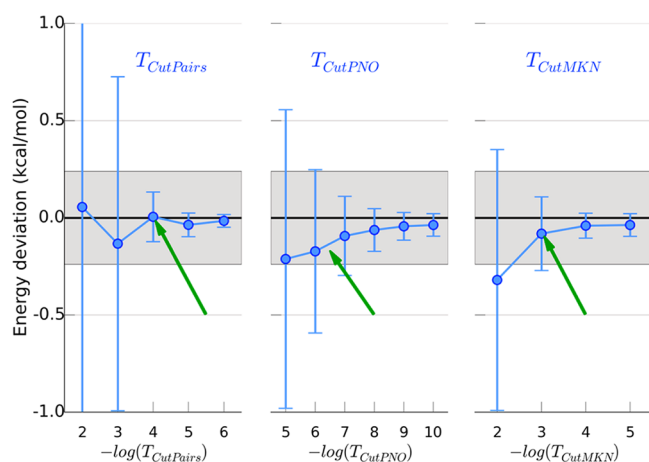


Figure 4. Convergence of the DLPNO-CCSD(T) method with respect to variation of T_{CutPairs} , T_{CutPNO} , and T_{CutMKN} . The average error and the associated standard deviation (shown as error bars) are computed with respect to the CCSD(T_0) for the FH data set. Basis set cc-pVDZ. (left panel) Convergence of T_{CutPairs} in the range from 10^{-2} to 10^{-6} ($T_{\text{CutPNO}} = 10^{-10}$ and $T_{\text{CutMKN}} = 0$). (central panel) Convergence of T_{CutPNO} in the range from 10^{-5} to 10^{-10} ($T_{\text{CutPairs}} = 0$ and $T_{\text{CutMKN}} = 0$). (right panel) Convergence of T_{CutMKN} in the range from 10^{-2} to 10^{-5} ($T_{\text{CutPairs}} = 0$ and $T_{\text{CutPNO}} = 10^{-10}$). The gray shadow highlights the region within 1 kJ/mol from the reference. With green arrows we denote the previous DLPNO-CCSD(T) default values.

−0.04 and 0.06 kcal/mol, respectively. The negligible remaining deviation is attributed to the use of the RI approximation adopted for DLPNO-CCSD(T) but not for CCSD(T_0).

The left panel in Figure 4 depicts the convergence with respect to T_{CutPairs} . For this threshold, the investigation covers the range from 10^{-2} Eh to 10^{-6} Eh. For all cases, the average error is found within the 1 kJ/mol region. With the tightest values of 10^{-5} Eh and 10^{-6} Eh, the accuracy limit of the method is approached (the maximum absolute deviation, MaxAD, is equal to 0.28 and 0.13 kcal/mol, respectively). This is consistent with the fact that, on average, more than 90% of the pairs are explicitly treated at the coupled cluster level. Conversely, a broader distribution of errors is observed for the looser thresholds due to the larger importance of the MP2 correction. For example, with $T_{\text{CutPairs}} = 10^{-3}$ Eh, the MAD is equal to 0.69 kcal/mol and deviations with respect to the reference up to 2.5 kcal/mol are observed. We note that with the previous default ($T_{\text{CutPairs}} = 10^{-4}$ Eh), the MaxAD is smaller than 0.5 kcal/mol.

In the central panel of Figure 4 the convergence of the results with respect to T_{CutPNO} follows the previously established pattern.^{40,60} In this case the range of values under consideration covers 4 orders of magnitude (10^{-5} to 10^{-9}). The convergence is smooth, and the larger deviation with respect to the reference is 1.2 kcal/mol already with $T_{\text{CutPNO}} = 10^{-6}$ (MAD = 0.34 kcal/mol). Finally, the right panel in Figure 4 shows the error associated with the variation of the T_{CutMKN} threshold. In this case, the parameter values in the range from 10^{-2} to 10^{-5} were investigated. For molecules of the size as these included in the FH data set, the convergence is achieved with $T_{\text{CutMKN}} = 10^{-4}$ (MAD and MaxAD are 0.06 and 0.26 kcal/mol), and with a T_{CutMKN} value of 10^{-3} , all deviations are smaller than 0.9 kcal/mol.

4.2. Exploring the Parameter Space. In the previous section, we examined the convergence of each of the thresholds in order to establish how the tightening of each parameter leads to the theoretical limit of the method. In this section, we will study the effect of the variation of these three thresholds on the accuracy of the DLPNO-CCSD(T) with respect to the CCSD(T_0). The goal of this survey is to determine optimal combinations of the thresholds that are consistent with a given requested accuracy.

Initially, the 51 reaction energies in the FH data set were considered and a detailed analysis of the results is shown in Supporting Information, Figure S3. As reported previously, at the method's limit ($T_{\text{CutPairs}} = 0$ Eh, $T_{\text{CutPNO}} = 10^{-10}$, and $T_{\text{CutMKN}} = 0$), the DLPNO results have essentially converged to the reference values. Using “real life” thresholds $T_{\text{CutPairs}} = 10^{-5}$, $T_{\text{CutPNO}} = 10^{-7}$, and $T_{\text{CutMKN}} = 10^{-4}$ and in combination with a full initial LMP2 calculation (see below), the MAD is 0.11 kcal/mol, the DLPNO-CCSD(T) results are well inside the demanding error goal of 1 kJ/mol, while the necessary calculations are still significantly faster than the canonical counterpart. It is interesting to note that with the same thresholds but using the semicanonical version of LMP2 correction, the results are only slightly worse and still inside the 1 kJ/mol area. Progressive loosening of the thresholds demonstrate the robustness of the method, in fact, with the setup suggested in the original publications^{60,61} ($T_{\text{CutPairs}} = 10^{-4}$, $T_{\text{CutPNO}} = 3.33 \times 10^{-7}$, and $T_{\text{CutMKN}} = 10^{-3}$), a MAD of 0.26 kcal/mol is obtained. In this case, the use of LMP2 method produces slightly worse results. Finally, in agreement with observed trends (see section 4.1), with less tight sets of thresholds, the errors on the reaction energies could reach up to 2 kcal/mol while the MAD is equal to 0.8 kcal/mol, still within chemical accuracy.

A similar analysis was conducted on the S66 data set, and the results are shown in Supporting Information, Figure S9. Once again, the DLPNO-CCSD(T) results converge to the reference values (MAD = 0.05 kcal/mol) at the method limit and the accuracy deteriorates (in average) only by one hundredth of a kcal/mol with a more realistic calculation ($T_{\text{CutPairs}} = 10^{-5}$, $T_{\text{CutPNO}} = 10^{-7}$, and $T_{\text{CutMKN}} = 10^{-4}$ and after a LMP2 guess).

In Supporting Information, Figure S4 and S10, statistical analysis for a series of combinations of T_{CutPairs} , T_{CutPNO} , and T_{CutMKN} as well as for the use of the LMP2 compared to its SC-LMP2 approximation is presented. Among these combinations, three sets of parameters were selected and will be referred to as LoosePNO, NormalPNO, and TightPNO (see Table 1 for details), where NormalPNO coincides with the previously chosen default values.^{40,60,61}

Table 1. Definition of the Three Default Thresholds Controlling the DLPNO

	T_{CutPairs}	T_{CutPNO}	T_{CutMKN}	recommended for
LoosePNO	10^{-3}	10^{-6}	10^{-3}	rapid estimates
NormalPNO	10^{-4}	3.33×10^{-7}	10^{-3}	general thermochemistry and thermochemical kinetics
TightPNO	10^{-5}	10^{-7}	10^{-4}	noncovalent interactions, conformational equilibria,

It is worthwhile to discuss the possible merits of LMP2 compared to SC-LMP2. For both data sets, the use of the full LMP2 in the construction of the guess and estimation of the corrections for weak pairs and PNO truncation leads to moderate improvements in the agreement with the reference values (ca. 0.05 kcal/mol on the MAD, TightPNO). For the less tight NormalPNO thresholds, the use of LMP2 improves the agreement compared to SC-LMP2 for the FH data set (MAD 0.13 and 0.26 kcal/mol, respectively) but slightly deteriorates the results for the S66 data set (MAD 0.38 and 0.24 kcal/mol). This observation can be rationalized by considering that with the NormalPNO setup, most of the electron pairs contributing to the nonbonding interactions have correlation energy below the $T_{\text{CutPairs}} = 10^{-4}$ Eh threshold. Therefore, they are considered weak pairs and their energy contribution is evaluated using MP2. As a consequence, the DLPNO–CCSD portion of the interaction energy is heavily dependent on T_{CutPairs} . With the NormalPNO settings, MP2 contributions account for 75% (on average) of the DLPNO–CCSD interaction energies, while only 10% MP2 contributions remain in TightPNO. As a consequence, the overestimation of the NormalPNO–DLPNO–CCSD interaction energies (Supporting Information, Figures S13 and S25) is due to the tendency of the MP2 method to overestimate the London dispersion energy.^{105,106} SC-LMP2 underestimates the LMP2 contributions and seemingly alleviates the issue. However, this is due to error cancellation and we therefore recommend the use of “TightPNO” settings when weak interactions are the target of the investigation.

As mentioned above, the cost of an (iterative) LMP2 calculation relative to the remaining coupled-cluster part in DLPNO–CCSD(T) is high. In fact, the LMP2 calculation time can easily dominate over the coupled cluster part. The reason for this behavior are the large domains that we choose to use in the DLPNO methods in order to ensure results that are accurate to within 99.8–99.9% of the correlation energy. In light of the high cost of the iterative LMP2 procedure with respect to the cost of the whole DLPNO–CCSD(T) calculation, we conclude that the computationally much more attractive SC-LMP2 method is adequate for the NormalPNO and LoosePNO setups. Whereas, motivated by the small improvements discussed earlier, we will investigate the use of LMP2 in connection with the TightPNO settings throughout this study.

The accuracy of the three setups presented in Table 1 have been investigated and the normal distributions of the errors computed with respect to the CCSD(T_0)/cc-pVTZ are shown in Figures 5 and 6 for the FH and S66 databases, respectively.

With the TightPNO setup, DLPNO–CCSD(T) delivers a set of reaction energies with an average error within about 0.5 kJ/mol (MAD = 0.13 kcal/mol) compared to CCSD(T_0) (green line). We consider this to be close to the practical accuracy limit of the method. Loosening of the thresholds results in a slightly larger error distribution (blue and red lines) and the MAD increases to 0.3 and 0.6 kcal/mol for NormalPNO and LoosePNO, respectively. Similar trends, i.e., the error distribution getting progressively sharper for the series LoosePNO, NormalPNO, and TightPNO, are observed for the melatonin (Supporting Information, Figure S14) and butane-1,4-diol data sets (Supporting Information, Figure S17 and S18). For the S66 database (Figure 6), a slightly different situation is observed. As for the other data sets, TightPNO guarantees an excellent accuracy with a sharp error distribution

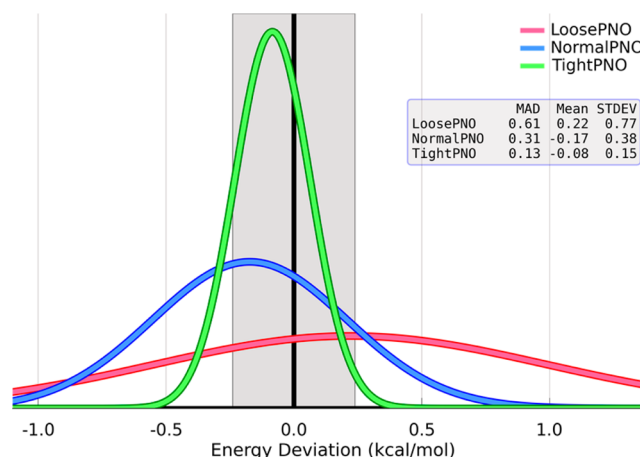


Figure 5. Comparison between DLPNO–CCSD(T)/cc-pVTZ and CCSD(T_0)/cc-pVTZ on the calculations of the reaction energies of the FH data set. Normal distributions of the errors are shown. The gray shadow highlights the region within 1 kJ/mol from the reference.

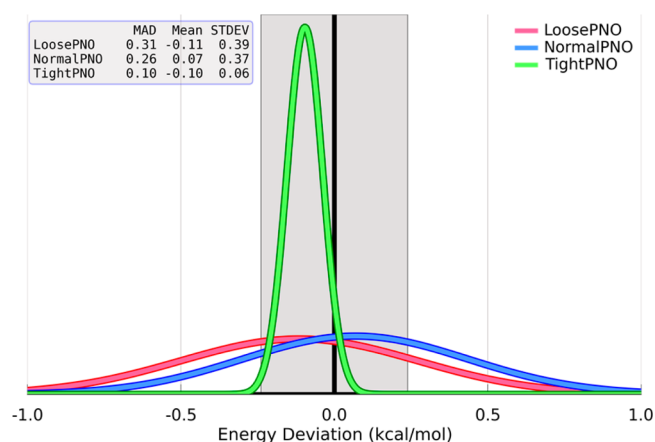


Figure 6. Comparison between DLPNO–CCSD(T)/cc-pVTZ and semicanonical CCSD(T_0)/cc-pVTZ on the calculations of the interaction energies of the S66 data set. Normal distributions of the errors are shown. The gray shadow highlights the region within 1 kJ/mol from the reference.

well within the 1 kJ/mol region; by contrast, NormalPNO and LoosePNO exhibit, on average, similar performances, which can be traced back to the error compensation discussed above. For a more detailed analysis of the results for each data set, we refer to sections 4.3.1–4.3.3.

The analysis for the four data sets confirms that the DLPNO–CCSD(T) method smoothly converges toward the CCSD(T_0) limit as the thresholds are tightened. Clearly, this comes with an increased computational cost. To illustrate this effect, we report the timings for the DLPNO and canonical calculations on the complex pentane...neopentane (reaction 37, S66). This is one of the largest systems investigated in this work, it comprises 64 correlated electrons and it requires 636 basis functions (cc-pVTZ). Remarkably, the DLPNO–CCSD(T) correlated calculation was completed in about 35 min (4 cores), approximately 2 orders of magnitude faster than the canonical counterpart. With the LoosePNO settings, a 35% reduction of the computational time was observed, whereas the accurate TightPNO calculation required ca. 200 min, approximately 6 times the time for the NormalPNO version. Furthermore, it is interesting to comment on the cost of the

triples excitations, in the series form LoosePNO to TightPNO, the cost for computing the (T) terms increases its relative weight going from 10% to 55%. Thus, at the tightest settings the relative cost of the (T_0) correction is about as expensive as the remaining calculations, similar to the canonical case. However, for larger molecules than the systems investigated here, the relative impact of the (T_0) correction diminishes owing to its perfectly linear scaling.⁶¹

Supporting Information, Figures S34 and S35 offer a graphical representation of the scaling of computational cost associated with the correlation energy calculation as a function of basis set size and number of atoms, respectively. From the figures one can conclude, the expected result, that the efficiency gains of DLPNO–CCSD(T) compared to the canonical counterpart are immense. Then especially over the 500 basis function region, calculations that were not possible at all with the canonical version become DLPNO–CCSD(T), especially with LoosePNO and NormalPNO, completely trivial.

An additional important aspect of the PNO methodology is the scaling of the method with the cardinal number. In principle, at a given threshold $T_{\text{CutPNO}} > 0$, the PNOs of a given electron pair converge toward a well-defined, finite set of pair natural orbitals as the basis set is approaching completeness. This means that past the integral transformation step, the timing of PNO based methods is almost independent of the basis set size. Because the integral transformation is the rate-limiting step in PNO based calculations, this still means that the basis set size has a significant influence on the wall clock times. However, this increase is not nearly as dramatic as for the canonical counterpart. To illustrate this point, in Figure 7, we

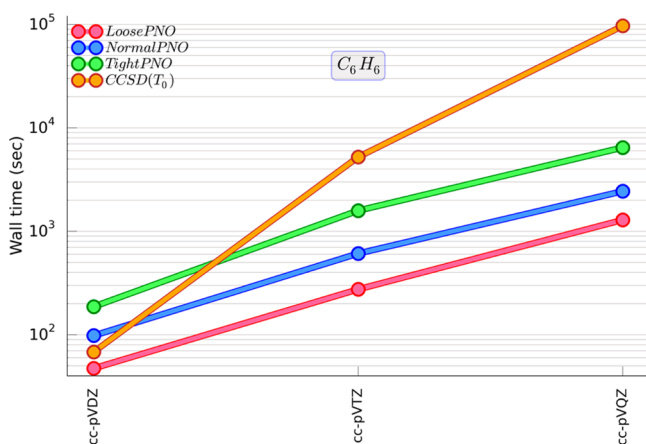


Figure 7. Scaling with the cardinal number for benzene.

use the benzene molecule as an example using the cc-pVnZ family of basis sets. In Supporting Information, Figure S37 we repeat the same procedure for formaldehyde that due to its smaller size allows us to perform even cc-pVSZ basis calculations.

CCSD(T_0) needs 77 times the time of cc-pVDZ when we use cc-pVTZ, and then this time needs to be multiplied by 19 to move to cc-pVQZ. Thus, as is well-known, going one cardinal number higher in the basis set costs almost 2 orders of magnitude additional computer time. For NormalPNO, the corresponding cost increases are factors of just 6 (cc-pVDZ \rightarrow cc-pVTZ) and 4 (cc-pVTZ \rightarrow cc-pVQZ). Thus, the advantages of DLPNO–CCSD(T) over canonical CCSD(T), and by inference other PNO methodologies as well, increase

enormously for the more accurate basis sets that one should use in correlated calculations in the first place. It is interesting to point out that even for a molecule as small as benzene where there is almost no locality to be used, DLPNO–CCSD(T) is almost 100 times faster than the canonical CCSD(T) code in conjunction with the cc-pVDZ basis set (the ORCA implementation is among the more efficient CCSD(T) codes in C_1 symmetry). The results are similar for formaldehyde. These results highlight the great benefits the DLPNO–CCSD(T) method realizes, i.e., there is no crossover with a canonical method and the efficiency does not fade when there is little or no locality. Within reasonable threshold ranges, the PNO methodology is always much more efficient than the corresponding canonical one.

We note in passing that these data were obtained in “production mode”, i.e., each calculation was sharing resources with competing jobs allocated on the same cluster node.

4.3. Balance of Computational Cost and Accuracy. In the previous section, we introduced three levels of tightness for the thresholds that control the DLPNO–CCSD(T) method. In this section, the results obtained for the different data sets are discussed in detail.

4.3.1. The FH Data Set. The accuracy of DLPNO–CCSD(T) for the 51 reaction energies of the FH data set is shown in Figure 8. To rationalize the energy deviation for each

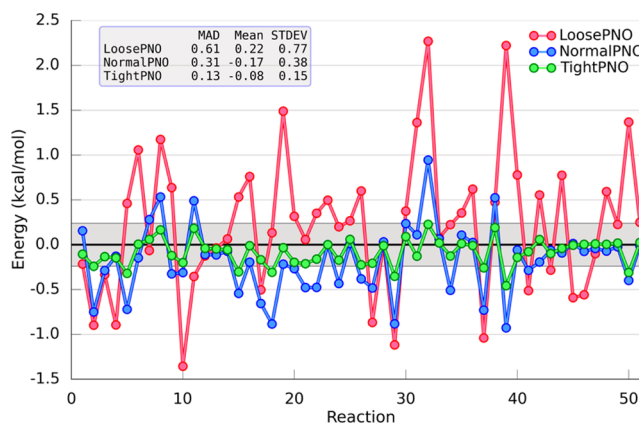


Figure 8. Deviations with respect to CCSD(T_0) for the FH data set obtained with LoosePNO, NormalPNO, and TightPNO DLPNO–CCSD(T). The gray shadow highlights the region within 1 kJ/mol. Basis set: cc-pVTZ.

of the combinations, the errors were partitioned into the contributions pertaining to the CCSD and (T) component of the energy (See Supporting Information, Figure S7). It is notable that with the TightPNO settings, both energy terms systematically approach the canonical results, giving rise to the excellent agreement with the reference as discussed before. With NormalPNO, both error distributions are only slightly broader but still very well centered around zero. Additionally, the details of CCSD and (T) components of the reaction energies for the NormalPNO setup (see Supporting Information, Figure S8) demonstrate that its accuracy does not rely on cancellation of errors because both the DLPNO–CCSD and DLPNO-(T) errors on the reactions energies have, in general, the same sign. Finally, the analysis of the energy components obtained with the LoosePNO set of parameters, confirms that a partial cancellation of errors is responsible for the small average error. Interestingly, within each of the three

levels of accuracy, a similar standard deviation is associated with the errors of the contribution of the CCSD correlation energy and that of the (T) correction to the reaction energy. This means that the method is well balanced and the total error is not dominated by a single term.

To further analyze the residual discrepancies with respect to the reference results, we investigated the absolute energies of each reactant and product. With the NormalPNO setup, on average, 99.9% of the basis set correlation energy is recovered by DLPNO–CCSD(T), in agreement with the results included in the original publications.^{60,61} For systems as the ones investigated for the FH data set, this translates into discrepancies in the absolute energy up to 2.5 kcal/mol. Upon taking energy differences, these deviations largely cancel because the DLPNO–CCSD(T) method always approaches the real correlation energy from above and the PNO errors are fairly smooth; however, some residual error is inherent to the method. For example, one of the largest errors is found for the isomerization $\text{CH}_2\text{C}_5\text{CH}_2 \rightarrow \text{heptatriyne}$ (reaction 32), here NormalPNO recovers 99.70% and 99.83% of the basis set correlation energy for reactant and product, respectively. In term of absolute energies, this corresponds to errors of 2.15 and 1.20 kcal/mol with respect to the reference results, hence the 0.95 kcal/mol discrepancy on the reaction energy. In Supporting Information, Figures S27 and S28, we explore the source of this error by plotting the pair correlation energies (in the region between 10^{-3} and 10^{-5} Eh) for both the reactant and product using canonical CCSD and DLPNO–CCSD. With the TightPNO setup (Supporting Information, Figure S27), almost all the electron pairs are above the $T_{\text{CutPairs}} = 10^{-5}$ threshold and are explicitly included in the coupled-cluster procedure. Therefore, only few (and small) LMP2 corrections are needed and they sum up to only 0.02 kcal/mol of the isomerization energy. Furthermore, the conservative thresholds for T_{CutPNO} and T_{CutMKN} ensure that the DLPNO pair correlation energy closely resemble the canonical counterpart, in summary, the discrepancy of the DLPNO methods with respect to CCSD is only 0.16 kcal/mol (this will be further reduced by the correction computed to account for the PNO truncation). Conversely, with NormalPNO settings (Supporting Information, Figure S28), the energies in the region between 10^{-4} and 10^{-5} Eh are obtained using the SC-LMP. In total, the MP2 contribution to the isomerization energy is equal to 0.25 kcal/mol. The larger MP2 component (and inherent error) and the slightly larger errors computed on the strong pair electron energy determine the total DLPNO error on the isomerization energy.

Finally, it is important recall that the reaction energy database stretches over a very large range. These results confirm the power of the DLPNO–CCSD(T) method because its accuracy is consistent for a wide variety of chemical reactions with reaction energies ranging from -0.1 to -150 kcal/mol. The excellent performance and computational efficiency demonstrated by DLPNO–CCSD(T) with the NormalPNO setup when applied to the FH database (MAD = 0.3 kcal/mol, maximum error <1.0 kcal/mol) confirm that is the setup of choice for the study of reaction energies as suggested in the original publications.^{60,61}

4.3.2. The S66 Data Set. Figure 9 presents a detailed analysis of the performance of DLPNO–CCSD(T) in the calculation of weak interactions for the S66 database. TightPNO setting delivers an excellent agreement with respect to the reference data, MAD is equal to 0.10 kcal/mol, and all the errors are

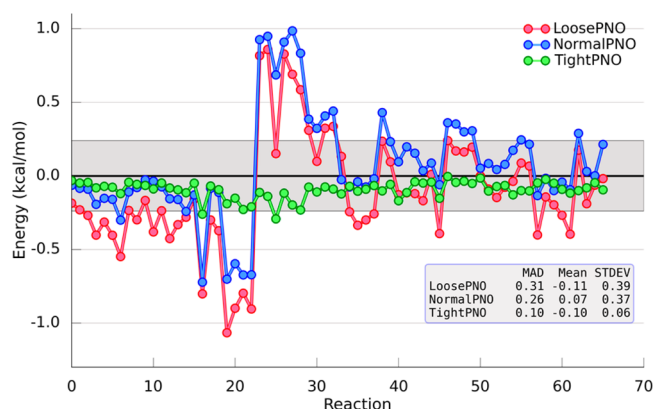


Figure 9. Deviations with respect to CCSD(T_0) for the S66 data set obtained with LoosePNO, NormalPNO, and TightPNO DLPNO–CCSD(T). The gray shadow highlights the region within 1 kJ/mol. Basis set: cc-pVTZ.

tightly clustered in the region kJ/mol. NormalPNO and LoosePNO show similar performance across the database and are found to be quite accurate (MAD 0.26 and 0.31 kcal/mol), with the largest discrepancies (ca. 1.0 kcal/mol) pertaining to systems dominated by π – π interactions (reactions 24–29: benzene dimer, pyridine dimer, uracil dimer, etc.).

Following up on this observation, we investigated how the nature of the nonbonding interaction (see section 3.1 for details) impacts the accuracy of NormalPNO calculations. For the electrostatically dominated molecular complexes, a slight underestimation of the interaction energies is observed but with overall small absolute deviations, whereas the binding energy of complexes dominated by the dispersion interactions is overestimated. Finally, these effects combine for the “mixed” complexes (Supporting Information, Figure S24). Furthermore, interaction energies were decomposed into their CCSD and (T) components. The (T) component was found to be independent of the nature of the interaction with NormalPNO DLPNO–(T) consistently underestimating the canonical counterpart (Supporting Information, Figure S26). On the contrary, DLPNO–CCSD with NormalPNO settings systematically overestimates the interactions in the “dispersion” and “mixed” subgroups but it gives very accurate results for the “electrostatic” one (Supporting Information, Figure S25). This can be rationalized by considering that with NormalPNO setup the nonbonding interactions rely on the MP2 corrections for the weak pairs and MP2 is known to perform well for H-bonded system but to overestimate π – π dispersion interactions.^{105,106} With the TightPNO setup, the importance of the MP2 correction in the interaction energy is greatly reduced (10% compared to 75% observed for the NormalPNO). This guarantees an excellent agreement between the TightPNO calculations and their canonical counterparts for all systems. The discrepancies on the CCSD component do not exceed 0.12 kcal/mol and the underestimations of the (T) contributions get significantly smaller (ca. 0.1 kcal/mol).

To further illustrate the method’s behavior, we will study here in detail the worst case, reaction 27, that presents an error of 0.94 kcal/mol using NormalPNO. In Table 2, we investigate the error on absolute energies and the corresponding reaction energy. It is noteworthy that none of the DLPNO setups leads to an estimation of the reaction energy based on huge cancellation of errors. In fact, errors on the absolute energies and on reaction energies have roughly the same order of

Table 2. Errors on Absolute and Reaction Energies for the Benzene–Pyridine Interaction (Reaction 27 of S66) As Function of the Level or Theory^a

	error on absolute energies			error on reaction energy
	benzene	pyridine	dimer	
SC-LMP2	−71.35	−71.02	−141.41	0.97
LMP2	−46.28	−43.37	−87.47	2.18
DLPNO–CCSD(T) LoosePNO	0.78	−0.22	1.43	0.86
DLPNO–CCSD(T) NormalPNO	−1.06	−1.27	−1.39	0.94
DLPNO–CCSD(T) TightPNO	−0.29	−0.37	−0.77	−0.12

^aAll values are given in kcal/mol. The reference reaction energy computed with canonical CCSD(T_0) is equal to −2.198 kcal/mol. Basis set: cc-pVTZ.

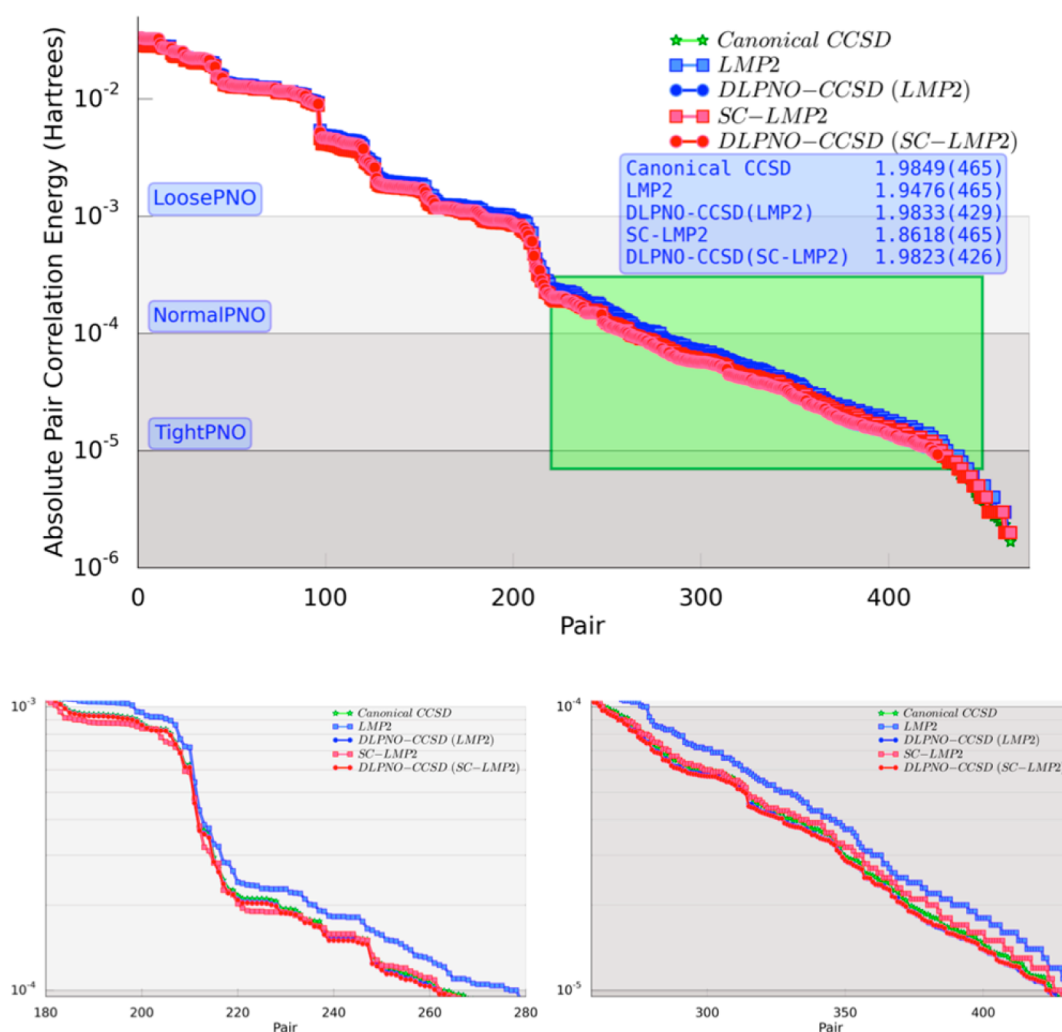


Figure 10. (top) Pair correlation energies for the product of reaction 27 (S66), using various setups. Blue frame: the sum of pair correlation energies and the number of strong pairs, in parentheses. Basis set: cc-pVTZ. Green shadow highlights the pairs responsible for the nonbonding interactions. (bottom) Zoom of the $[10^{-3}; 10^{-4}]$ and the $[10^{-4}; 10^{-5}]$ regions.

magnitude. All the DLPNO absolute energies are within 1.5 kcal/mol from their canonical counterparts, whereas at MP2 the error can reach up to 140 kcal/mol. This is achieved with excellent computational efficiency: NormalPNO and TightPNO calculations are 52 and 15 times faster than the corresponding CCSD(T_0)/cc-pVTZ calculation (60 h on four processors).

We subsequently focused on what causes the increase in error upon loosening of the thresholds. The pair correlation energies computed with different setups are shown in Figure

10. The green highlighted region is important in the context of weak interactions because this region contains no electron pairs in the reactants but is densely populated with “intermolecular electron pairs” in the product. Furthermore, we recall that the pairs above the T_{CutPairs} (values 10^{-3} , 10^{-4} , and 10^{-5} for LoosePNO, NormalPNO, and TightPNO, respectively) are included in the coupled-cluster procedure. At CCSD level pairs between 10^{-3} and 10^{-4} Eh account for 0.03327 Eh (1.68%) of the correlation energy. Regardless of the guess used, the DLPNO–CCSD pair energies are practically identical and the

cumulative error is less than 0.001 Eh. We note that the electron pairs with in this region are considered weak with the LoosePNO setup. The pairs in the 10^{-4} and 10^{-5} Eh region are responsible for 0.00642 Eh of correlation energy (0.32% of the total). In spite of their small absolute contribution, this region dominates the intermolecular interaction energy. The cumulative contributions amount to 4.03 kcal/mol of the interaction energy. When TightPNO settings are used, DLPNO–CCSD delivers very accurate energies for these pairs and the cumulative errors are negligible regardless of the MP2 flavor used as guess: 0.09 kcal/mol (LMP2) or 0.13 kcal/mol (SC-LMP2). It is interesting to note (Figure 10) that the CCSD portion of the DLPNO–CCSD energy is barely affected by the choice of either the SC-MP2 or the LMP2 guess. This means that the very small differences that exist between the PNOs produced by the two methods do not impact the accuracy of the energies. The only thing that matters for the choice of the guess method is the estimate of the correlation energy brought in by the weak pairs that are eventually not treated by CCSD.

Overall we conclude that the TightPNO setup (despite the increased computational cost) is the preferred choice when weak interactions are the focus of the investigation and high accuracy is demanded. The results obtained in this way faithfully follow the canonical results and do not rely on cancellation of errors of any kind.

4.3.3. The Melatonin and Butane-1,4-diol Data Sets. Statistical analysis of DLPNO–CCSD(T) deviations from the reference results on the relative energy of the conformers of melatonin and butane-1,4-diol are shown in Figures 11 and 12, respectively.

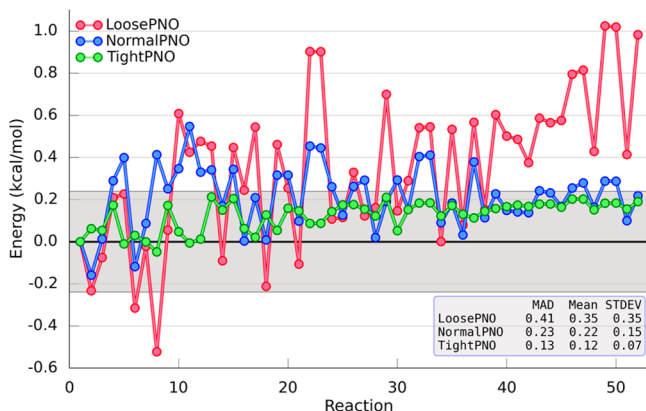


Figure 11. Deviations with respect to CCSD(T_0) for the melatonin conformers data set obtained with LoosePNO, NormalPNO, and TightPNO DLPNO–CCSD(T). The gray shadow highlights the region within 1 kJ/mol. Basis set: cc-pVDZ. See Supporting Information, Figures S14–S16, for statistical analysis and VZT basis set data.

In both cases, with the TightPNO settings, the deviations from the reference results are very small and slight deterioration of the agreement is observed for melatonin upon loosening of the thresholds (NormalPNO). However, the MAD error remains smaller than 1 kJ/mol. Furthermore, we note that the maximum absolute deviation is slightly above the 0.5 kcal/mol in just one case, whereas 50% of the remaining errors are within the kJ/mol region. The realization of this level of accuracy for both melatonin (whose conformational energies are dictated by the interplay of hydrogen bond and quadru-

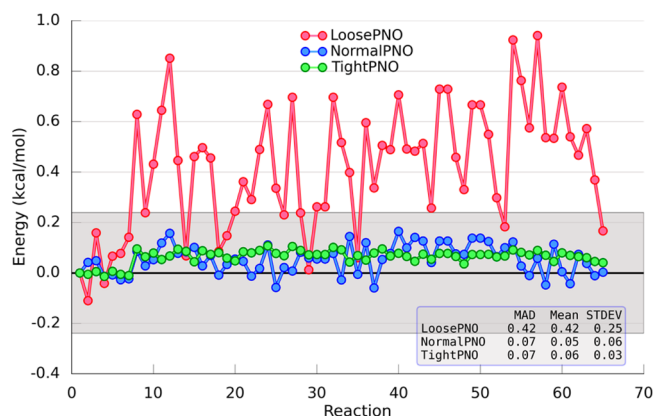


Figure 12. Deviations with respect to CCSD(T_0) for the butane-1,4-diol conformers data set obtained with LoosePNO, NormalPNO, and TightPNO DLPNO–CCSD(T). The gray shadow highlights the region within 1 kJ/mol. Basis set: cc-pVTZ. See Supporting Information, Figures S17–S19, for statistical analysis and cc-pVDZ data.

pole–dipole aromatic–amide interactions) and the “mixed” subgroup of the S66 set suggests that conformational energies of molecular systems where dispersion and electrostatic interactions coexist can be described with an error of less than 0.5 kcal/mol with the default DLPNO settings. If higher accuracy is needed, one can rely on the TightPNO settings. With this setup, DLPNO–CCSD(T) provide results that are consistently found within 1 kJ/mol from the CCSD(T_0) counterparts. Finally, with the LoosePNO settings, the relative conformational energies are slightly overestimated (MAD of ca. 0.4 kcal/mol) for both melatonin and butane-1,4-diol. Nevertheless, even with these settings, all errors are found within the 1 kcal/mol region.

One final aspect to take into consideration is whether the energetic ordering of the conformers is correctly reproduced by the different approximations. By comparing the conformational energy obtained with the different DLPNO setups with the reference values, it was verified that order of the isomers is well reproduced with the TightPNO setup. With NormalPNO some almost isoenergetic conformers (within 0.15 kcal/mol) were swapped. Finally, we note that even with LoosePNO the correct ordering is obtained most of the time (Supporting Information, Figure S32).

4.3.4. A Real-Life Organometallic Example: The Grubbs Catalyst. In this section, we will consider a model system¹⁰⁷ for the Grubbs metathesis reaction. This system has previously been the subject of benchmark calculations by Zhao and Truhlar¹⁰⁷ using conventional coupled cluster methods and by two of us¹⁰⁸ through explicitly correlated coupled cluster theory.^{109,110}

The various points on the potential energy surface are sketched in Figure 13.

Relative energies using different PNO cutoff criteria have been collected in Table 3. As the reference point of the energies, we have taken $2 + \text{C}_2\text{H}_4$. The basis sets considered is the def2-TZVP Weigend–Ahlichs basis set,¹¹¹ which includes a Stuttgart–Cologne relativistic energy-consistent pseudopotential¹¹² for elements heavier than krypton. In our present calculations, we have chosen to freeze the Ru(4s,4p) orbitals, as the RI basis sets¹¹³ for def2-TZVP will be inadequate in the “semi-core” region for Ru.

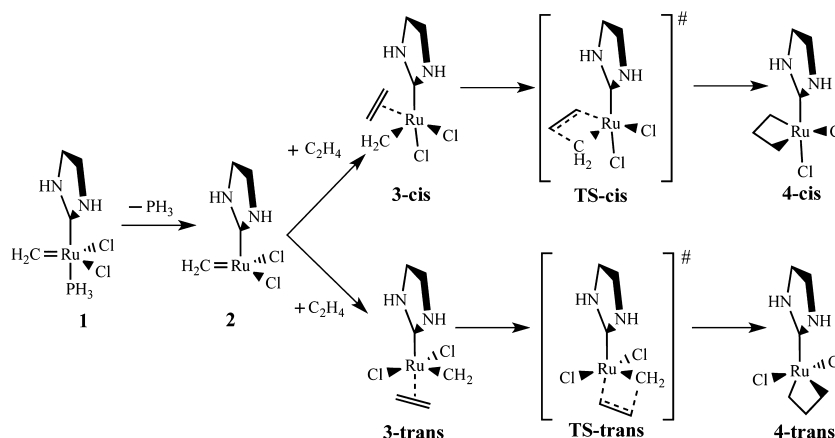


Figure 13. Stationary points on the Grubbs metathesis reaction pathway.

Table 3. RMSD (kcal/mol) of Relative Energies for the Grubbs Metathesis Model in Figure 13 Relative to CCSD(T_0) Results^a

	LoosePNO		NormalPNO	TightPNO		CCSD(T)
NrMP2 Pairs_Trip	1	2	1	1	1	3
T_{CutTNO}	10^{-7}	10^{-7}	10^{-7}	10^{-7}	10^{-8}	0
CCSD component	3.55	3.55	0.30	0.28	0.28	0
(T_0) triples	1.91	0.48	0.56	0.24	0.14	0.29
CCSD(T_0) total	2.07	3.37	0.80	0.52	0.41	0.29
wrt to CCSD(T)	1.82	3.09	1.03	0.77	0.65	0

^aThe def2-TZVP basis set was used throughout.

As the benchmark, one might use canonical CCSD(T) calculations. However, because the DLPNO–CCSD(T) model is effectively an approximation to CCSD(T_0) rather than to CCSD(T) proper, we have also obtained semicanonical CCSD(T_0) values. Relative energies differ by up to 0.40 kcal/mol (RMS difference 0.29 kcal/mol) between CCSD(T) and CCSD(T_0), hence DLPNO–CCSD(T) relative energies need not be converged to better than that, relatively speaking.

Considering first the CCSD contribution separately, we find the LoosePNO criteria to be wholly unacceptable, causing an RMS error in the relative CCSD energies of 3.6 kcal/mol, with individual errors ranging from 1 to 5 kcal/mol. We note that between 67% and 72% of pairs are being screened out with the LoosePNO criteria. With the NormalPNO criteria (where “only” between 30 and 36% of pairs are being screened out), the RMS deviation from the canonical CCSD numbers improves by an order of magnitude to 0.30 kcal/mol, with individual errors now ranging from 0.1 to 0.5 kcal/mol. Switching to TightPNO does not improve the RMSD, although the largest individual error (for TScis) is now reduced to 0.4 kcal/mol.

Turning now to (T) by itself, LoosePNO causes an error of almost 2 kcal/mol. Interestingly, this can be reduced to just 0.48 kcal/mol by setting NrMP2Pairs_Trip=2 (which admits triples involving two weak pairs, rather than the default of one): however, in view of the large error in the CCSD component, this is not helpful for the present problem. With the NormalPNO criteria, the error in (T) is reduced to 0.56 kcal/mol RMS, the largest individual error being 0.77 kcal/mol. T_{CutTNO} is the selection threshold for triples natural orbitals (TNOs). The TNOs for a given contribution to the triples energy are constructed from the sum of the pair densities of the three pairs that contribute to that term in the (T) expression. Hence, the TNOs span the union of the spaces that the three

PNO sets span.⁶¹ With TightPNO criteria, a further reduction to 0.24 kcal/mol RMSD is achieved: by tightening the (T) summation cutoff T_{CutTNO} to 10^{-8} from the default of 10^{-7} , this number can be further reduced to 0.14 kcal/mol. However, in view of the fact that the (T_0) limit itself differs by 0.29 kcal/mol RMS from canonical values, the additional computational cost does not appear to be warranted. Additional tightening of T_{CutTNO} to 10^{-9} is found to have negligible effect on the relative energies.

Considering now the CCSD(T) numbers in the aggregate, we can make the same observations. LoosePNO entails an RMS deviation of 2 kcal/mol (with individual errors reaching almost 4 kcal/mol) and is thus only acceptable for crude initial prototyping: in fact, these error statistics are inferior to what can be obtained¹⁰⁸ using some dispersion-corrected DFT methods. NormalPNO yields RMSD = 0.80 kcal/mol with a largest error (for TScis) of 1.3 kcal/mol, which would be acceptable for most application studies. At the hefty computational “surcharge” entailed by TightPNO, this can be further reduced to 0.52 kcal/mol RMSD (largest 0.83 kcal/mol for TScis); a further reduction to 0.41 kcal/mol is achievable by tightening T_{CutTNO} by a factor of 10. The T_0 approximation itself, it should be recalled, deviates by 0.29 kcal/mol RMS from canonical CCSD(T). If we take the canonical CCSD(T) energies as a reference, then NormalPNO still meets the RMSD = 1 kcal/mol test, while TightPNO with tightened T_{CutTNO} can achieve RMSD = 0.65 kcal/mol.

4.4. Extrapolation to the Complete Basis Set limit. In this section, we investigate the accuracy of DLPNO–CCSD(T) at the basis set limit by means of extrapolation techniques. For this purpose, we used the direct extrapolation^{96–98} of the energies obtained with cc-pVDZ and cc-pVTZ.

$$E^{\text{CBS}}(X, Y) = \frac{E_{\text{HF}}(Y)e^{-\alpha\sqrt{X}} - E_{\text{HF}}(X)e^{-\alpha\sqrt{Y}}}{e^{-\alpha\sqrt{X}} - e^{-\alpha\sqrt{Y}}} + \frac{X^\beta E_{\text{corr}}(X) - Y^\beta E_{\text{corr}}(Y)}{X^\beta - Y^\beta}$$

where $E_{\text{HF}}(X)$ is the Hartree–Fock energy obtained with the basis set with cardinal number X , 2 for cc-pVDZ, and 3 for cc-pVTZ, $E_{\text{corr}}(X)$ similarly is the corresponding correlation energy and α, β constants depending on the basis sets. It is important to note that we do not advocate for the use of the cc-pVDZ/cc-pVTZ extrapolation to obtain accurate results as it has been shown that this procedure is less robust than the bare cc-pVTZ results owing to the poor quality of the cc-pVDZ basis set.⁵⁹ However, the scope of this section is to investigate if extrapolated values obtained with DLPNO–CCSD(T) behave similar to their canonical counterparts. Because the accuracy observed for the three setups proposed for DLPNO–CCSD(T) is roughly independent of the basis set (see Figure 5 and Supporting Information, Figure S5 or Figure 8 and Supporting Information, Figure S6 for cc-pVDZ and cc-pVTZ, respectively), it is reasonable to expect that the complete basis set limit extrapolated DLPNO results will have similar errors as the ones documented above. In Figure 14, normal distributions

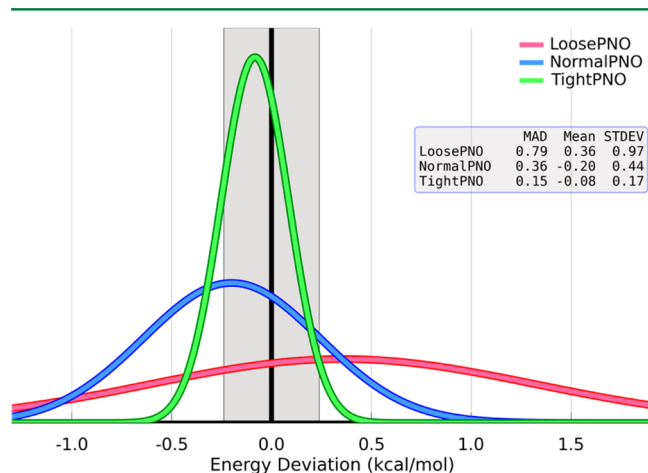


Figure 14. Effect of the complete basis set extrapolation (D/T). Normal distribution of the errors obtained with LoosePNO, NormalPNO, and TightPNO DLPNO–CCSD(T) with respect to CCSD(T_0) for the FH data set. The gray shadow highlights the region within 1 kJ/mol.

of the CBS data computed on the FH data set for the three sets of thresholds are presented (Supporting Information, Figure S33 for details). As expected, the extrapolated values show approximately the same accuracy observed for the parent data, e.g., a MAD of 0.36 and 0.15 kcal/mol is found for NormalPNO and TightPNO, respectively. This, in turn, validates direct extrapolation of DLPNO–CCSD(T) results. Similarly, the excellent accuracy obtained for the conformational energies of butane-1,4-diol with either cc-pVDZ and cc-pVTZ is reflected in the extrapolated data (Supporting Information, Figures S20 and S21).

The observation that the extrapolation retains the same accuracy observed for parent data supports that DLPNO–CCSD(T) extrapolated results using larger basis sets (e.g., cc-pVTZ/cc-pVQZ) will also be a good approximation for the canonical counterparts.

4.5. Additional Considerations. During the implementation and initial testing of the perturbative triples correction for the DLPNO method, it was concluded that although weak pairs are excluded from the explicit coupled-cluster iterations, they have to be considered when compiling the list of triple excitations to ensure accurate results.⁶¹ Specifically, it was found to be important to consider corrections for the triple excitations that involve two strong pairs and one weak pair. In this work, the effect of including one additional class of triples (consisting of one strong pair and two weak pairs) was investigated. We conclude that the calculation of these additional triples provides only marginal improvements to the accuracy (MAD 0.22 vs 0.25 kcal/mol, see Supporting Information, Figure S22). In the light of the minor enhancement and considering the significant increase ($\sim 2\times$) of the computational cost associated with the DLPNO-(T), we do not advocate for the inclusion of this class of triple excitations for routine applications.

In the original publication, a parameter controlling the atoms entering in the pair domains ($T_{\text{CutDeloc}} = 10^{-1}$) was introduced.⁶⁰ The effect of tightening the threshold was investigated, and it was found that enlarging the domain size by ($T_{\text{CutDeloc}} = 10^{-2}$) have virtually no effects if the TightPNO settings are already in place. For example, considering the reaction 24 in the FH data set: dimethyloxirane + $\text{H}_2\text{O} \rightarrow$ butandiol (reference value 23.45 kcal/mol, CCSD(T_0)/cc-pVTZ), reaction energy of 23.26 and 23.27 kcal/mol are obtained with TightPNO and TightPNO + $T_{\text{CutDeloc}} = 10^{-2}$, respectively. In the case of NormalPNO calculations, it is observed that the small additional correlation energy terms are primarily due to basis set superposition errors. In fact, counterpoise corrected relative energies do not depend on the T_{CutDeloc} threshold. For example, for the uracil dimer (reaction 26 in the S66 data set, counterpoise corrected CCSD(T_0)/cc-pVTZ = 7.40 kcal/mol), NormalPNO and NormalPNO + $T_{\text{CutDeloc}} = 10^{-2}$ return 10.64 and 11.05 kcal/mol, respectively; however, after counterpoise correction, the interaction energy converges (8.05 and 7.97 kcal/mol, respectively).

In Figure 15, we show results compiled for the cyclohexane molecule in the def2-TZVP basis. From this plot it becomes evident that the convergence of the correlation energy with respect to the energy selected PNOs as well as the correlation energy recovered per PNO is worse than in the occupation number selection. On the basis of these results and further test calculations, we have decided to not further follow the idea of energy selection.

We further investigated whether the spin-component scaled variants of the MP2 scheme (SCS-MP2)⁸⁷ can improve the accuracy of DLPNO–CCSD(T). SCS-MP2 aims at improving the accuracy of second-order Møller–Plesset perturbation theory by separate scaling of parallel- and antiparallel-spin pair correlation energies.⁸⁷ The modifications necessary to obtain the SCS-MP2 are cost-free, and this scheme can be implemented both for SC-LMP2 and LMP2. We note that the benchmarks included in this manuscript focus on relative energies (reaction energies, weak interactions, isomerization energies). As discussed, such quantities should not depend on the MP2 variant used in the initial guess and PNO construction. The MP2-based corrections (weak pairs and truncation of the PNO spaces) are, however, important to reproduce the total energy of a system to high accuracy, but they are expected to largely cancel out for relative energies.

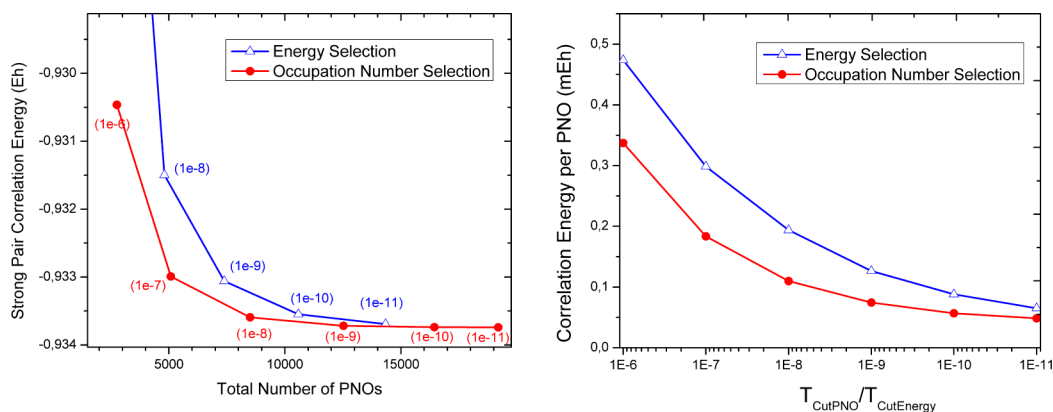


Figure 15. PNO selection results for the cyclohexane molecule in the def2-TZVP basis. On the left, the recovered correlation energy is shown as a function of the number of selected PNOs (selection thresholds in parentheses; the energy selection threshold is given in Eh). On the right the correlation energy recovered per selected PNO is shown as a function of the selection threshold.

Ideally, improvements of the final results are due to an optimal partitioning of strong and weak pairs rather than rely on an empirical tuning of the weak pairs contributions. Indeed, a statistical analysis of the deviation with respect to the CCSD(T_0) demonstrated that the use of SCS-RI-MP2 does not increase the accuracy of the predicted reaction energies of the FH data set (Supporting Information, Figure S23). We therefore will refrain from further investigating empirical schemes such as SCS-MP2 as they distract from the first-principles nature of the DLPNO-CCSD(T) method while not leading to better accuracy.

Finally, throughout this work we investigated the use of the full LMP2 method compared to the simpler SC-LMP2 variant in the initial guess, PNO construction and perturbative correction for PNO and weak-pair errors. On the basis of the extensive results assembled in this study, we do not advocate the use of full-LMP2 in the DLPNO-CCSD(T) framework because in our opinion the minor improvements in accuracy, which may or may not be statistically significant, do not justify the significantly higher computational cost associated with full LMP2 over SC-LMP2.

5. CONCLUSIONS

In this work, we have investigated how far the accuracy of the DLPNO-CCSD(T) approach can realistically be pushed for chemical applications that involve the calculation of reaction energies and weak intra- and intermolecular interactions. It is evident that for achieving higher accuracy of the local scheme relative to its canonical counterpart, more computer time must be invested. It should also be remembered that the results should always be viewed in the context of a given application. What we have addressed here is the error in the electronic energy at the CCSD(T) level for a given basis set. In practice, there will be inaccuracies in the electronic energies arising from the basis set and from effects beyond triple excitations. Furthermore, there will be errors arising from inaccuracies in the employed geometries, shortcomings of the treatment of the environment, of the zero-point energy, of the entropic contributions to the free energy, or of system dynamics, to name only a few. In many cases, the cumulative errors from these various sources will turn out to be larger than the errors in the electronic energies. Hence, to best utilize the results of this study, it is important to have well-defined accuracy goals. In our opinion, for most intents and purposes, it is sufficient to

calculate reaction energies to an accuracy better than 1 kcal/mol and weak interactions to an accuracy better than about 0.3 kcal/mol.

These are goals that have been difficult to achieve previously. However, it appears that the DLPNO-CCSD(T) method is able to comply with the requested accuracy while still realizing huge computational advantages over canonical coupled-cluster theory. In this study, we have demonstrated that this accuracy holds for a wide variety of chemical reactions as well as for weak intra- and intermolecular interaction energies. The melatonin data set of 51 conformers was a specific example, where it was demonstrated that an accuracy of about 0.1 kcal/mol can be achieved. In general, for systems up to the size of these described here, the achievable accuracy limit appears to be about 0.2–0.3 kcal/mol. We have defined three sets of default thresholds called LoosePNO, NormalPNO, and TightPNO. For medium sized molecules, the calculations with the TightPNO settings are 3–4 times more expensive than the ones with the LoosePNO settings. LoosePNO corresponds to the combination $T_{\text{CutPairs}} = 10^{-3}$, $T_{\text{CutPNO}} = 10^{-6}$, and $T_{\text{CutMKN}} = 10^{-3}$. This set of thresholds leads to MAD of 0.6 kcal/mol in the calculation of the FH reaction energies or 0.3 kcal/mol for the S66 data set. Clearly, this level of accuracy is sufficient for initial screening or exploration of a potential energy surface. With the NormalPNO defaults, all the errors in the energy reaction data set fall within the 1 kcal/mol region (MAD = 0.3 kcal/mol), making this choice accurate for most computational applications. Finally, with the TightPNO setup, MAD in the reaction energy data set drops to 0.13 kcal/mol, making this the level of choice for very accurate calculations, as well as for some noncovalent interactions where 0.3 kcal/mol would be a nontrivial percentage of the interaction energy. For a prototype organometallic reaction problem (the Grubbs metathesis), LoosePNO was found to yield unacceptable errors, while NormalPNO meets the 1 kcal/mol test and TightPNO can further improve on this if desired.

Although the quoted accuracy is established for systems up to ca. 30 atoms, it should be mentioned that it is not difficult to construct pathological systems for which the errors of any local correlation method will be larger than the quoted averages. One case will be met, for example, if one is studying the intermolecular interaction of two very long, parallel running hydrocarbon chains. It is evident that for each point of contact between the two chains, there will be a small error. However, many small errors of the same sign will eventually

add up to a sizable discrepancy that, once the chains are long enough, will also exceed the error limits given here. We believe that such situations are unavoidable. They will require a special treatment to compensate for the systematic errors. For general purpose, large-scale chemical applications the DLPNO-CCSD(T) method is a reliably accurate and efficient choice.

■ ASSOCIATED CONTENT

■ Supporting Information

CCSD(T) vs CCSD(T0), FH, S66, melatonin, butane-1,4-diol datasets, complete basis set extrapolation, additional considerations, figures for different basis sets and additional analysis. This material is available free of charge via the Internet at <http://pubs.acs.org>.

■ AUTHOR INFORMATION

Corresponding Author

*E-mail: Frank.Neese@cec.mpg.de.

Funding

F.N. gratefully acknowledges the DFG-SPP 1601, Cluster of Excellence RESOLV (Ruhr-Universität Bochum) as well as the Max Planck Society for financial support. Research at Weizmann was supported by the Minerva Foundation, Munich, Germany, by the Helen and Martin Kimmel Center for Molecular Design, and by the Lise Meitner-Minerva Center for Computational Quantum Chemistry.

Notes

The authors declare no competing financial interest.

■ ACKNOWLEDGMENTS

J.M.L.M. thanks Dr. Irena Efremenko for helpful discussions.

■ REFERENCES

- (1) Bartlett, R. J.; Musial, M. *Rev. Mod. Phys.* **2007**, *79*, 291.
- (2) Klopper, W.; Noga, J.; Koch, H.; Helgaker, T. *Theor. Chem. Acc.* **1997**, *97*, 164.
- (3) Constans, P.; Ayala, P. Y.; Scuseria, G. E. *J. Chem. Phys.* **2000**, *113*, 10451.
- (4) Pitonak, M.; Holka, F.; Neogrady, P.; Urban, M. *J. Mol. Struct. – Theochem* **2006**, *768*, 79.
- (5) Forner, W.; Ladik, J.; Otto, P.; Cizek, J. *Chem. Phys.* **1985**, *97*, 251.
- (6) Forner, W. *Chem. Phys.* **1987**, *114*, 21.
- (7) Rosciszewski, K.; Doll, K.; Paulus, B.; Fulde, P.; Stoll, H. *Phys. Rev. B* **1998**, *57*, 14667.
- (8) Stoll, H. *Physical Rev. B: Condens. Matter* **1992**, *46*, 6700.
- (9) Fedorov, D. G.; Kitaura, K. *J. Chem. Phys.* **2005**, *123*, 134103.
- (10) Li, W.; Li, S. H. *J. Chem. Phys.* **2004**, *121*, 6649.
- (11) Kristensen, K.; Hoyvik, I. M.; Jansik, B.; Jorgensen, P.; Kjaergaard, T.; Reine, S.; Jakowski, J. *Phys. Chem. Chem. Phys.* **2012**, *14*, 15706.
- (12) Ziolkowski, M.; Jansik, B.; Kjaergaard, T.; Jorgensen, P. *J. Chem. Phys.* **2010**, *133*, 014107.
- (13) Li, W.; Piecuch, P.; Gour, J. R.; Li, S. H. *J. Chem. Phys.* **2009**, *131*, 114109.
- (14) Li, W.; Piecuch, P. *J. Phys. Chem. A* **2010**, *114*, 8644.
- (15) Rolik, Z.; Kallay, M. *J. Chem. Phys.* **2011**, *135*, 104111.
- (16) Friedrich, J.; Walczak, K. *J. Chem. Theory Comput.* **2013**, *9*, 408.
- (17) Friedrich, J.; Tew, D. P.; Klopper, W.; Dolg, M. *J. Chem. Phys.* **2010**, *132*, 164114.
- (18) Friedrich, J.; Hanrath, M.; Dolg, M. *J. Chem. Phys.* **2007**, *126*, 154110.
- (19) Saebo, S.; Tong, W.; Pulay, P. *J. Chem. Phys.* **1993**, *98*, 2170.
- (20) Saebo, S.; Pulay, P. *Annu. Rev. Phys. Chem.* **1993**, *44*, 213.
- (21) Saebo, S.; Pulay, P. *Chem. Phys. Lett.* **1985**, *113*, 13.
- (22) Saebo, S.; Pulay, P. *J. Chem. Phys.* **1988**, *88*, 1884.
- (23) Saebo, S.; Pulay, P. *J. Chem. Phys.* **1987**, *86*, 914.
- (24) Schutz, M.; Yang, J.; Chan, G. K.; Manby, F. R.; Werner, H. J. *J. Chem. Phys.* **2013**, *138*, 054109.
- (25) Schutz, M.; Werner, H. J. *J. Chem. Phys.* **2001**, *114*, 661.
- (26) Schutz, M.; Werner, H. J. *Chem. Phys. Lett.* **2000**, *318*, 370.
- (27) Schutz, M.; Rauhut, G.; Werner, H. J. *J. Phys. Chem. A* **1998**, *102*, 5997.
- (28) Schutz, M.; Hetzer, G.; Werner, H. J. *J. Chem. Phys.* **1999**, *111*, 5691.
- (29) Yang, J.; Chan, G. K.; Manby, F. R.; Schutz, M.; Werner, H. J. *J. Chem. Phys.* **2012**, *136*, 144105.
- (30) Werner, H. J.; Schutz, M. *J. Chem. Phys.* **2011**, *135*, 144116.
- (31) Scuseria, G. E.; Ayala, P. Y. *J. Chem. Phys.* **1999**, *111*, 8330.
- (32) Maslen, P. E.; Dutoi, A. D.; Lee, M. S.; Shao, Y. H.; Head-Gordon, M. *Mol. Phys.* **2005**, *103*, 425.
- (33) Subotnik, J. E.; Head-Gordon, M. *J. Chem. Phys.* **2005**, *123*, 64108.
- (34) Subotnik, J. E.; Sodt, A.; Head-Gordon, M. *J. Chem. Phys.* **2006**, *125*, 074116.
- (35) Tew, D. P.; Helmich, B.; Hättig, C. *J. Chem. Phys.* **2011**, *135*, 074107.
- (36) Hättig, C.; Tew, D. P.; Helmich, B. *J. Chem. Phys.* **2012**, *136*, 204105.
- (37) Helmich, B.; Hättig, C. *J. Chem. Phys.* **2013**, *139*, 084114.
- (38) Yang, J.; Kurashige, Y.; Manby, F. R.; Chan, G. K. *J. Chem. Phys.* **2011**, *134*, 044123.
- (39) Huntington, L. M.; Hansen, A.; Neese, F.; Nooijen, M. *J. Chem. Phys.* **2012**, *136*, 064101.
- (40) Neese, F.; Wennmohs, F.; Hansen, A. *J. Chem. Phys.* **2009**, *130*, 114108.
- (41) Neese, F.; Hansen, A.; Liakos, D. G. *J. Chem. Phys.* **2009**, *131*, 064103.
- (42) Staemmler, V.; Jungen, M. *Chem. Phys. Lett.* **1972**, *16*, 187.
- (43) Staemmler, V. *Theor. Chim. Acta* **1973**, *31*, 49.
- (44) Kutzelnigg, W.; Staemmler, V.; Hoheisel, C. *Chem. Phys.* **1973**, *1*, 27.
- (45) Gelus, M.; Ahlrichs, R.; Staemmler, V.; Kutzelnigg, W. *Theor. Chim. Acta* **1971**, *21*, 63.
- (46) Driessle, F.; Ahlrichs, R.; Staemmler, V.; Kutzelnigg, W. *Theor. Chim. Acta* **1973**, *30*, 315.
- (47) Werner, H. J.; Meyer, W. *Mol. Phys.* **1976**, *31*, 855.
- (48) Meyer, W.; Rosmus, P. *J. Chem. Phys.* **1975**, *63*, 2356.
- (49) Meyer, W. *Theor. Chim. Acta* **1974**, *35*, 277.
- (50) Meyer, W. *J. Chem. Phys.* **1973**, *58*, 1017.
- (51) Dykstra, C. E.; Schaefer, H. F.; Meyer, W. *J. Chem. Phys.* **1976**, *65*, 5141.
- (52) Ahlrichs, R.; Kutzelnigg, W. *J. Chem. Phys.* **1968**, *48*, 1819.
- (53) Edmiston, C.; Krauss, M. *J. Chem. Phys.* **1966**, *45*, 1833.
- (54) Edmiston, C.; Krauss, M. *J. Chem. Phys.* **1965**, *42*, 1119.
- (55) Krause, C.; Werner, H. J. *Phys. Chem. Chem. Phys.* **2012**, *14*, 7591.
- (56) Anoop, A.; Thiel, W.; Neese, F. *J. Chem. Theory Comput.* **2010**, *6*, 3137.
- (57) Liakos, D. G.; Neese, F. *J. Chem. Theory Comput.* **2011**, *7*, 1511.
- (58) Liakos, D. G.; Hansen, A.; Neese, F. *J. Chem. Theory Comput.* **2011**, *7*, 76.
- (59) Liakos, D. G.; Neese, F. *J. Phys. Chem. A* **2012**, *116*, 4801.
- (60) Riplinger, C.; Neese, F. *J. Chem. Phys.* **2013**, *138*, 034106.
- (61) Riplinger, C.; Sandhoefer, B.; Hansen, A.; Neese, F. *J. Chem. Phys.* **2013**, *139*, 134101.
- (62) Sparta, M.; Riplinger, C.; Neese, F. *J. Chem. Theory Comput.* **2014**, *10*, 1099.
- (63) Sparta, M.; Neese, F. *Chem. Soc. Rev.* **2014**, *43*, 5032.
- (64) Curtiss, L. A.; Raghavachari, K.; Redfern, P. C.; Pople, J. A. *J. Chem. Phys.* **2000**, *112*, 7374.
- (65) Curtiss, L. A.; Redfern, P. C.; Raghavachari, K. *J. Chem. Phys.* **2005**, *123*, 124107.

- (66) Dybala-Defratyka, A.; Paneth, P.; Pu, J. Z.; Truhlar, D. G. *J. Phys. Chem. A* **2004**, *108*, 2475.
- (67) Nachimuthu, S.; Gao, J. L.; Truhlar, D. G. *Chem. Phys.* **2012**, *400*, 8.
- (68) Pu, J. Z.; Truhlar, D. G. *J. Phys. Chem. A* **2005**, *109*, 773.
- (69) Tishchenko, O.; Truhlar, D. G. *J. Phys. Chem. Lett.* **2012**, *3*, 2834.
- (70) Zhao, Y.; Truhlar, D. G. *J. Chem. Theory Comput.* **2005**, *1*, 415.
- (71) Zheng, J. J.; Zhao, Y.; Truhlar, D. G. *J. Chem. Theory Comput.* **2007**, *3*, 569.
- (72) Zhao, Y.; Gonzalez-Garcia, N.; Truhlar, D. G. *J. Phys. Chem. A* **2005**, *109*, 2012.
- (73) Pitonak, M.; Neogady, P.; Cerny, J.; Grimme, S.; Hobza, P. *ChemPhysChem* **2009**, *10*, 282.
- (74) Hujo, W.; Grimme, S. *Phys. Chem. Chem. Phys.* **2011**, *13*, 13942.
- (75) Huenerbein, R.; Schirmer, B.; Moellmann, J.; Grimme, S. *Phys. Chem. Chem. Phys.* **2010**, *12*, 6940.
- (76) Grimme, S.; Ehrlich, S.; Goerigk, L. *J. Comput. Chem.* **2011**, *32*, 1456.
- (77) Goerigk, L.; Grimme, S. *Phys. Chem. Chem. Phys.* **2011**, *13*, 6670.
- (78) Antony, J.; Grimme, S. *Phys. Chem. Chem. Phys.* **2006**, *8*, 5287.
- (79) Goerigk, L.; Grimme, S. *J. Chem. Theory Comput.* **2011**, *7*, 291.
- (80) Friedrich, J.; Hänchen, J. *J. Chem. Theory Comput.* **2013**, *9*, 5381.
- (81) Rezáč, J.; Riley, K. E.; Hobza, P. *J. Chem. Theory Comput.* **2011**, *7*, 2427.
- (82) Jurecka, P.; Sponer, J.; Cerny, J.; Hobza, P. *Phys. Chem. Chem. Phys.* **2006**, *8*, 1985–1993.
- (83) Duan, G.; Smith, V. H.; Weaver, D. F. *J. Phys. Chem. A* **2000**, *104*, 4521.
- (84) Csontos, J.; Kalman, M.; Tasi, G. *J. Mol. Struct.—Theochem* **2003**, *640*, 69.
- (85) Csontos, J.; Kalman, P.; Tasi, G.; Kalman, M.; Murphy, R. F.; Lovas, S. *J. Comput. Chem.* **2008**, *29*, 1466.
- (86) Fogueri, U. R.; Kozuch, S.; Karton, A.; Martin, J. M. L. *J. Phys. Chem. A* **2013**, *117*, 2269.
- (87) Grimme, S. *J. Chem. Phys.* **2003**, *118*, 9095.
- (88) Boys, S. F. *Rev. Mod. Phys.* **1960**, *32*, 296.
- (89) Hylleraas, E. A. *Z. Phys.* **1930**, *65*, 209.
- (90) Pulay, P.; Saebo, S. *Theor. Chim. Acta* **1986**, *69*, 357.
- (91) Neese, F. *Wires Comput. Mol. Sci.* **2012**, *2*, 73.
- (92) Dunning, J. T. H. *J. Chem. Phys.* **1989**, *90*, 1007.
- (93) Kendall, R. A.; Dunning, T. H.; Harrison, R. J. *J. Chem. Phys.* **1992**, *96*, 6796.
- (94) Boys, S. F.; Bernardi, F. *Mol. Phys.* **1970**, *19*, 553.
- (95) Weigend, F.; Kohn, A.; Hättig, C. *J. Chem. Phys.* **2002**, *116*, 3175.
- (96) Klopper, W.; Kutzelnigg, W. *J. Mol. Struct.—Theochem* **1986**, *28*, 339.
- (97) Halkier, A.; Helgaker, T.; Jørgensen, P.; Klopper, W.; Koch, H.; Olsen, J.; Wilson, A. K. *Chem. Phys. Lett.* **1998**, *286*, 243.
- (98) Helgaker, T.; Klopper, W.; Koch, H.; Noga, J. *J. Chem. Phys.* **1997**, *106*, 9639.
- (99) Hansen, A. Ph.D. Thesis. Rheinischen Friedrich-Wilhelms-Universität Bonn, 2012, (<http://hss.ulb.uni-bonn.de/2012/2976/2976.htm>).
- (100) Haas, T.; Jaeger, B.; Weber, R.; Mitchell, S. F.; King, C. F. *Appl. Catal., A* **2005**, *280*, 83.
- (101) Zeng, A. P.; Sabra, W. *Curr. Opin. Biotechnol.* **2011**, *22*, 749.
- (102) Jesus, A. J. L.; Rosado, M. T. S.; Reva, I.; Fausto, R.; Eusebio, A. E. S.; Redinha, J. S. *J. Phys. Chem. A* **2008**, *112*, 4669.
- (103) Dijk, D. J.; Cajochen, C. *J. Biol. Rhythm* **1997**, *12*, 627.
- (104) Carpentieri, A.; de Barboza, G. D.; Areco, V.; Lopez, M. P.; de Talamoni, N. T. *Pharmacol. Res.* **2012**, *65*, 437.
- (105) Cybulski, S. M.; Lytle, M. L. *J. Chem. Phys.* **2007**, *127*, 141102.
- (106) Jurecka, P.; Sponer, J.; Cerny, J.; Hobza, P. *Phys. Chem. Chem. Phys.* **2006**, *8*, 1985.
- (107) Zhao, Y.; Truhlar, D. G. *J. Chem. Theory Comput.* **2009**, *5*, 324.
- (108) Kesharwani, M. K.; Martin, J. M. L. *Theor. Chem. Acc.* **2014**, *133*, 1452.
- (109) Hättig, C.; Klopper, W.; Kohn, A.; Tew, D. P. *Chem. Rev.* **2012**, *112*, 4.
- (110) Kong, L.; Bischoff, F. A.; Valeev, E. F. *Chem. Rev.* **2012**, *112*, 75.
- (111) Weigend, F.; Ahlrichs, R. *Phys. Chem. Chem. Phys.* **2005**, *7*, 3297.
- (112) Dolg, M.; Cao, X. *Chem. Rev.* **2012**, *112*, 403.
- (113) Hättig, C. *Phys. Chem. Chem. Phys.* **2005**, *7*, 59.